Geochemical Journal, Vol. 39, pp. 427 to 439, 2005

Reconnaissance of soil gas composition over the buried fault and fracture zone in southern Taiwan

CHING-CHOU FU,[1] TSANYAO FRANK YANG,[1]* VIVEK WALIA[1,2] and CHENG-HONG CHEN[1,3]

[1]Department of Geosciences, National Taiwan University, P.O. Box 13-318, Taipei 106, Taiwan
[2]National Center for Research on Earthquake Engineering, Taipei 106, Taiwan
[3]National Applied Research Laboratories, Taipei 106, Taiwan

(*Received December 18, 2004; Accepted August 17, 2005*)

The soil-gas method is based on the principle that faults and/or fractures are highly permeable pathways in rock formation where gases can migrate upward from the deep crust and/or mantle and retain their deep-source signatures in the soil cover. This method is adopted because it can give results in short time and at low costs. In this work, soil-gas compositions are measured and synthesized in conjunction with the geological, geophysical and geomorphological information along the Chaochou Fault, which is considered as an active fault in southern Taiwan.

More than 500 soil-gas samples were collected along 18 traverses crossing the observed structures and analyzed for He, CO_2, CH_4, O_2 + Ar and N_2. The results show that both helium and carbon dioxide concentrations in the soil gas have anomalous values at the specific positions in each of the traverses. The trace of these positions coincides with the N-S trending faults and/or fractures, that is, the postulated trend and pattern of the faults in southern Taiwan. Hence, helium and carbon dioxide are useful index gases in this area.

Based on the helium and carbon dioxide concentrations of the soil gases, at least three components are required to explain the observed variations. In addition to the atmospheric air component, two gas sources can be recognized. One is the deep crust component, exhibiting high He and CO_2 concentrations, and considered as best indicator for the surface location of fault/fracture zones in the region. The other component could be a shallower gas source with high CO_2 concentration, and low He concentration. Moreover, helium isotopic compositions of representative samples vary from 0.52 to 1.05 *Ra* (the $^3He/^4He$ ratio of air), illustrating that most samples have soil air component and may be mixed with some crustal component but no significant input of mantle component. Carbon isotopic composition ($\delta^{13}C$) of carbon dioxide in the soil samples vary from –11.8 to –23.4‰, which could be the result of mixing of organic and limestone components. Both helium and carbon isotopic results support the multiple gas sources in studied area. Meanwhile, continuous monitoring indicates that soil gas variations at fault zone may be closely related to the local crustal stress and hence, is suitable for further monitoring on fault activities.

Keywords: soil gas, active fault, Chaochou Fault, helium, carbon dioxide, Taiwan

INTRODUCTION

Taiwan is located on the boundary between Eurasia plate and Philippine Sea plate. As a result of the continuous stress and collision, Taiwan is densely faulted (Lin *et al*., 2000). Therefore, one of the major tasks for disaster mitigation is to delineate the distribution of active faults. So far most of research has been based on geophysical techniques, and studies of trenches, geomorphology, and structural geology (e.g., Hu *et al*., 2001; Lee *et al*., 2001; Lin *et al*., 2002; Chen *et al*., 2003, 2004). In contrast, geochemical methods were rarely used for these kinds of problems in Taiwan. The study of soil gases has already been used since long for the exploration of petroleum (e.g., Blunt *et al*., 1993; Belt and Rice, 2002), uranium mineralization (e.g., Reimer and Otton, 1976; Butt and Gole, 1986; Gole *et al*., 1986), geothermal reservoirs (e.g., Roberts *et al*., 1975; Hinkle, 1978; Corazza *et al*., 1993), and earthquake prediction (e.g., King, 1980; Virk and Singh, 1993; Al-Hilal and Mouty, 1994, Chyi *et al*., 2002, 2005; Walia *et al*., 2005b; Yang *et al*., 2005b), etc. Besides, the feasibility of the soil gas method to explore blind faults and fractures has also been mentioned (Gregory and Durrance, 1985; Etiope and Lombardi, 1995; Fytikas *et al*., 1999; Toutain and Baubron, 1999; Guerra and Lombardi, 2000; Baubron *et al*., 2001; Walia *et al*., 2005a).

In the eighties, some researchers have tried to apply the soil gas method to prospect the fault distributions in

*Corresponding author (e-mail: tyyang@ntu.edu.tw)

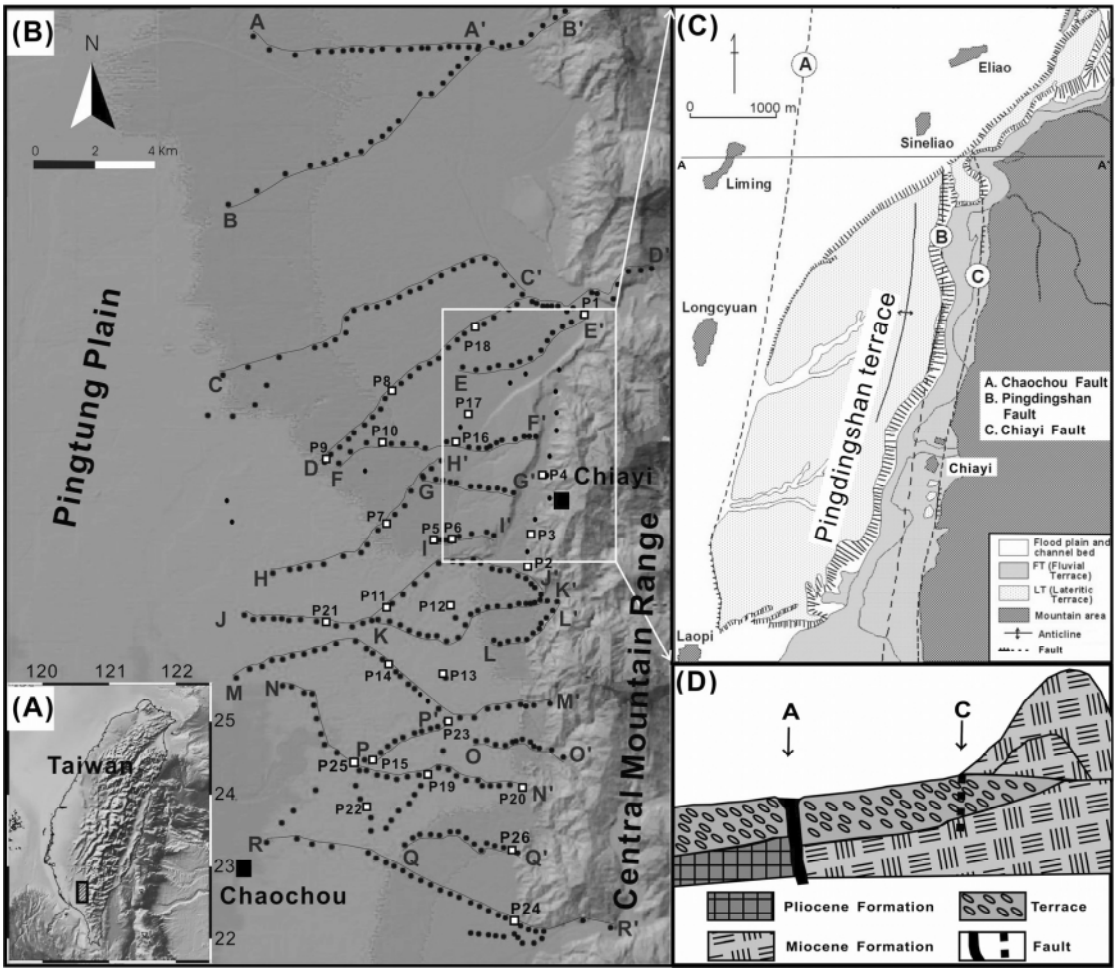

Fig. 1. Sampling sites and simplified structural map of the studied area. (A) Studied area is marked as rectangle in southern Taiwan and enlarged shown as (B), which shows the sampling sites. Black dots indicate the sample site for soil gas collection; hollow-squares indicate the sample site for additional measurements of helium and carbon isotopes. In total 18 transverses (profiles A to R) were investigated in this study. The marked rectangle is enlarged shown as (C), which displays the structural distribution of faults and geomorphic surface features around the Chaochou Fault zone (modified from Shih et al., 1984). (D) Sketched A–A′ profile, marked in (C), of north segment of the Chaochou Fault. Arrows indicate the major faults shown in (C) (modified from Chang, 1986).

Taiwan (e.g., Huang *et al*., 1986; Weng, 1988). However, the results were not satisfactory due to limitations in the analytical technique. With the improved instrumentation available at present, it is possible to analyses soil gas compositions instantaneously in the field which allow fast and accurate identification of the gas anomaly. Helium and carbon dioxide soil gas data can be used to better understand the influence of buried structures on gas migration and concentration in the subsurface (e.g., Toutain and Baubron, 1999). If anomalies of soil gas compositions can be matched with geophysical and geological data, the surface location of blind faults/fractures can be determined more accurately.

Helium (^{4}He) is produced in the subsurface environment by the radioactive decay of U and Th contained in the rocks. Helium, a light noble gas, has unique characteristics: it is chemically inert, non-biogenic, highly mobile, relatively insoluble in water and radioactively stable (Reimer, 1980; Ozima and Podosek, 2002). These characteristics give helium some advantages over other gases commonly measured in soil surveys such as carbon dioxide and methane, which may also have an organic source.

Carbon dioxide is thought to be the major component of endogenic gas and a suitable carrier for trace gases (Gregory and Durrance, 1985; Etiope and Lombardi,

1995; Yang *et al*., 2003b). It occurs in many geological environments and originates primarily from the decomposition of organic matter, metamorphism of carbonate sediments and mantle degassing. Sugisaki (1983) observed that in some cases high carbon dioxide concentrations did not occur only exclusively along a fault plane, but also in association with related fractures.

The present study is aimed to apply the soil gas method to the Chaochou (CC) Fault of the Pingtung region, South Taiwan (Fig. 1). This region is characterized by complicated fault and fracture systems, and is less populated which makes soil gas sampling easier. Lineations constructed from anomalous helium and carbon dioxide soil degassing in this region is correlated with the geological and geomorphological features. These data can also be used to assess the influence of crustal activity on soil gas degassing.

Geological Setting of the Area

Alluvium is the widely distributed formation in the area under consideration and comprises mainly uncemented sand, mud, gravels and pebbles. The N-S trend of the CC Fault has been considered as the major geological structure in the area. The Fault is located on a structure boundary between the Pingtung Plain and central mountain ranges in southern Taiwan (Lin *et al*., 2000). In addition to the CC Fault, the Chiayi (CY) Fault was also identified to share the same fault structures in the area (Fig. 1C) (Shih *et al*., 1984).

Based on the study of satellite images, Wang (1976) concluded that the so-called CC Lineament could be the surface trace of the CC Fault. Furthermore, Shih *et al*. (1984, 1986) suggested that the CC Fault is an active fault based on the geomorphological studies. The distribution of gravity anomalies also shows a N-S trend which is consistent with the surface trace of CC Fault (Hsieh, 1970). The gravity values show an increase in their values with depth from the Pingtung Plain toward the Central Mountain Range, revealing that on both sides of the Fault rocks of different compositions are juxtaposed. Furthermore, the data suggest that there is a high angle thrust fault plane dipping to east 75–80 degrees. Compiling the seismic and drill core data, Chiang (1971) concluded that the Wanlong (WL) Fault, which is located at the southwest of the CC Fault, cuts through the western flank of the CC Anticline. Yu *et al*. (1983) deduced from microearthquakes and gravity data that the dip angle of the CC Fault is about 70 to 80 degrees. Based on the observation of trenching and field investigation, Chang (1986) concluded that the surface distribution of the CC Fault should be located at west side of the topographic lineament of the foothill, where most people believed it was the fault scarp of CC Fault (Fig. 1D).

Methodology

Principle

Generally, gas compositions are entirely different in air and deep-crust derived components. The latter usually exhibit higher concentration of He, Rn, CO_2 and CH_4 which will diffuse upward to the surface and mix with the air. Thus soil gas compositions usually are mixtures of these two components. Deep faults or fractures that underlie the surface may provide conduits for the gases that migrate upward from the deep crust or mantle and produces deep source signatures in the soil gases (e.g., Ciotoli *et al*., 1999; Guerra and Lombardi, 2000; Baubron *et al*., 2001; Yang *et al*., 2003b; Walia *et al*., 2005a). Therefore, anomalous soil gas compositions could be able to reveal the presence of faults and/or fractures below the surface. Based on this principle, the soil gas technique is commonly applied to detect buried faults or trails of faults that cannot be recognized in the filed due to, e.g., human activity and/or natural events.

Sampling and analysis

Published topographic and geologic maps have been taken in consideration to develop a sampling grid for the areas of the probable fault distribution. Sampling intervals varied from 50 to 400 m. More than 500 soil gas samples were collected during the time period from February 2004 to August 2004 along the 18 transverse profiles and are shown in the Fig. 1B.

For soil-gas sampling, a hollow steel probe of 3 cm diameter and 130 cm length with a disposable sharp awl, which can make steel probe favorable for drilling into the soil and prevent soil from blocking the probe, was inserted into the soil at the depth of about 100 cm. A thin solid billet then was inserted into the hollow steel probe to displace the awl. A hand-pump through a specially designed rubber tube (with two filters: one is for dust and another one is for mist) connected with the hollow steel probe is used to collect gas into sample bag and bottle. The sample bottle, which is made of potassium glass to preserve helium gas from escaping by diffusion, is used for further helium isotope analysis (Yang *et al*., 2005a).

Helium and other gases like carbon dioxide, methane, argon, oxygen and nitrogen from the sample bags were analyzed within a few hours after sampling using a helium leak detector (ASM100HDS, Alcatel) and micro gas chromatography (CP4900, Varian), respectively. Helium, neon and other noble gases concentration and their isotopic ratios were analyzed by a noble gas mass spectrometer (Micromass 5400). The observed $^3He/^4He$ ratios were calibrated against atmospheric standard gas and were expressed relative to *Ra*, where *Ra* is the air $^3He/^4He$ ratio of 1.39×10^{-6}. The overall error of the measured ratio, including the analytical errors of the sam-

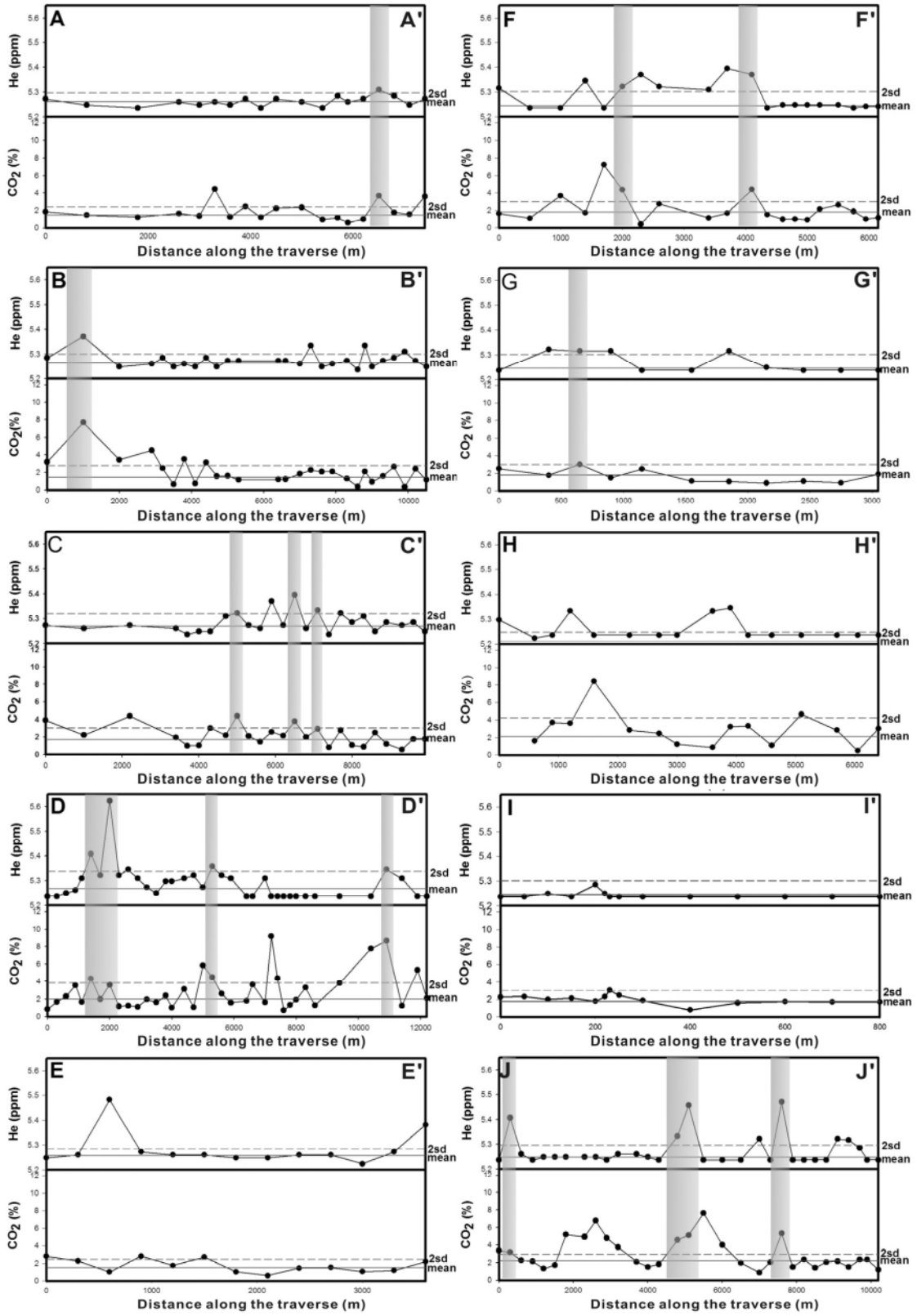

Fig. 2. Variations of He and CO_2 concentrations of soil gases for each profile marked in Fig. 1B. Profiles A–J shown in (A), and (B) for profiles K–R. The horizontal solid line indicates the mean value; dash line indicates the threshold ($+2\sigma$) for anomalous concentration on the profiles. The solid triangles represent the values higher than threshold value. Shading marks the area where the anomalous helium concentrations coincide with carbon dioxide anomalies.

ple and the working standard gas, and long-term variations of standard, was less than 2.5% (Yang *et al*., 2005a). After purification of the soil gas samples by traps held at liquid N_2 and ethanol-dry ice temperature, carbon dioxide for carbon isotopic was analyzed using a Finnigan MAT mass spectrometer. Measured $^{13}C/^{12}C$ ratios are expressed in the delta (δ) notation, as parts per thousand (‰) deviation from the international standard, PDB. The experimental error on the carbon isotopic ratios was ~0.1‰ (Hsieh, 2000).

In general, helium has constant concentration (5.24 ppm) in atmospheric air and background soil gases. So we collected surface air as a background value to compare with soil gas samples at the same time for all profiles.

Result and Discussion

From the analysis of the collected samples it has been found that oxygen plus argon, and nitrogen do not show

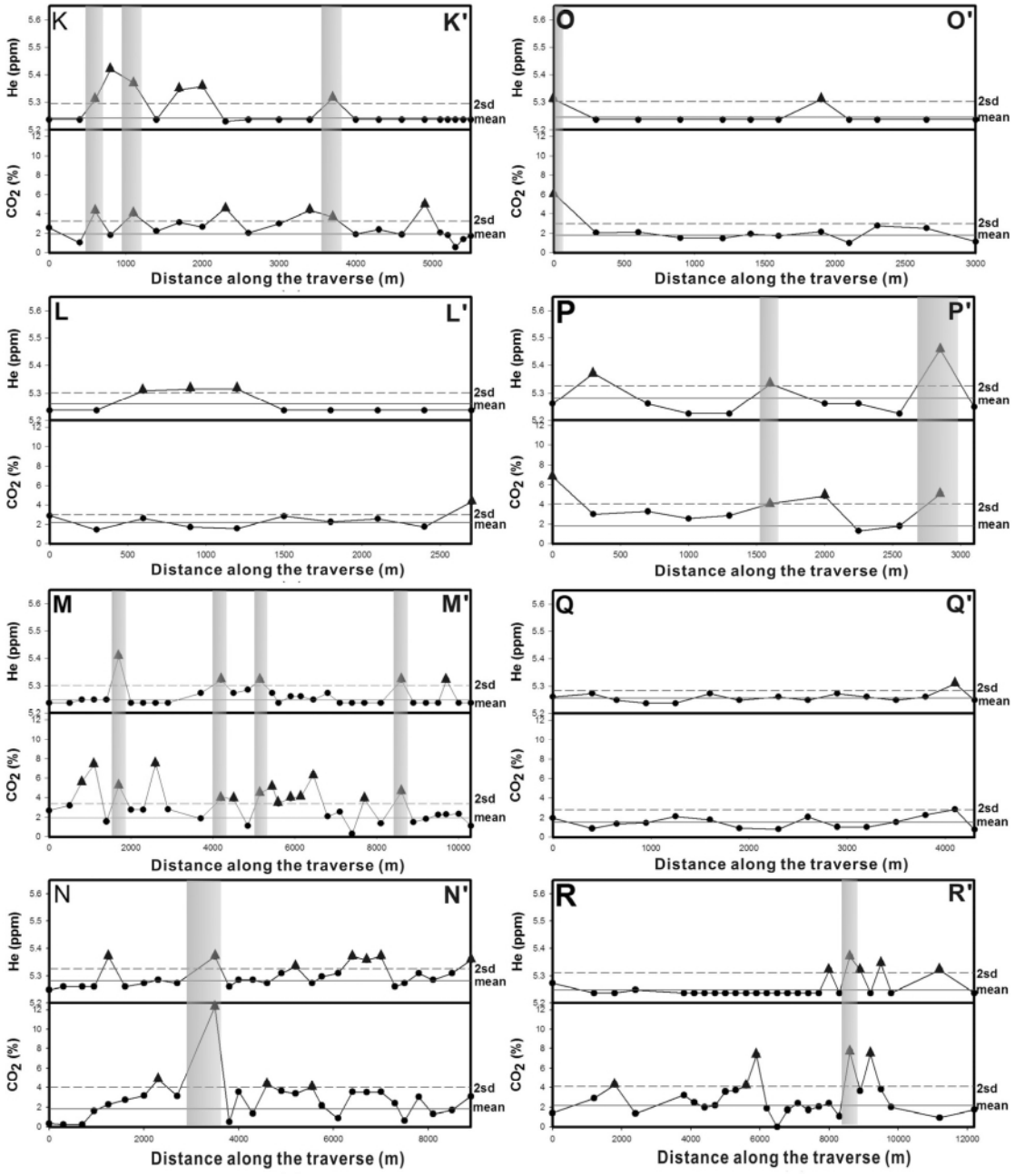

Fig. 2. (continued).

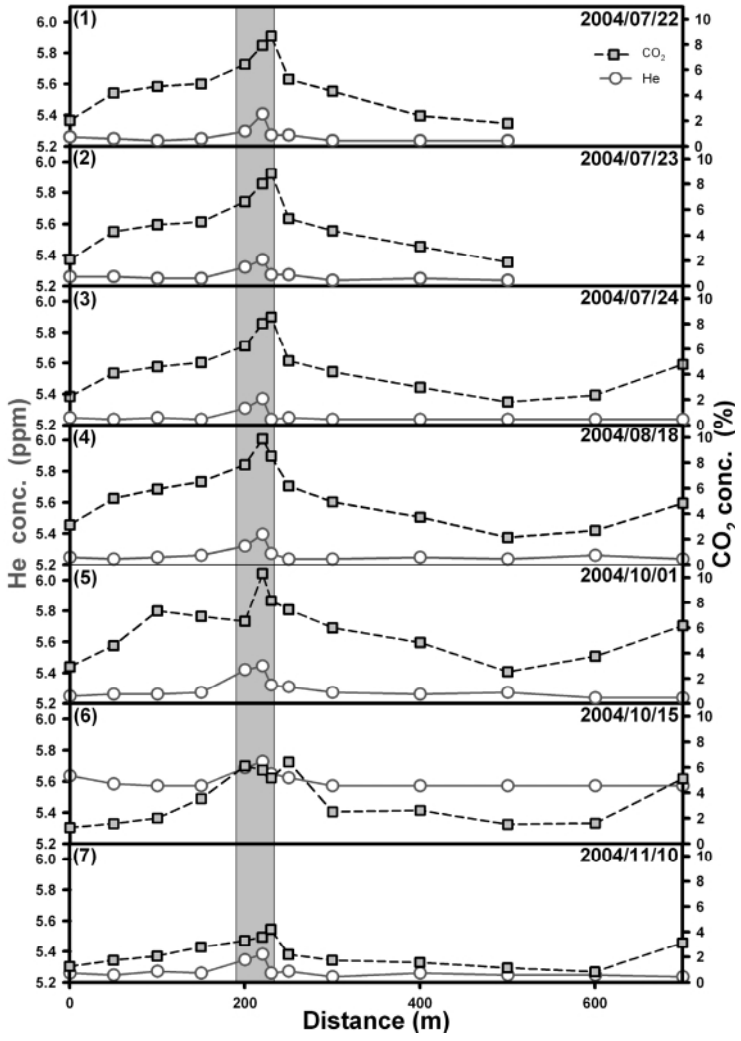

Fig. 3. Variations of He and CO_2 concentrations of soil gases for profile I during the time window 22nd July to 10th November, 2004. Shadowed area indicates the location of anomalous concentration, considered as the probable fault position.

any distinct variation and cannot be used as an indicator gas for tracing faults in this study. However, these gases and atmospheric air background values are helpful to check the success of sample collection. In addition, no methane has been found in the investigated area, so there will be no further discussion on it.

Recognition of anomalous concentrations

The samples were collected under same conditions within one-two days for each profile to eliminate possible meteorological effects on the soil gas compositions. Threshold values, which are used for recognizing anomalous concentrations of soil gas data, were calculated using the mean plus two standard deviation of the trimmed data set for each profile in present study. The mean values of soil gas compositions were quite constant for different profiles and ranged from 5.21 to 5.28 ppm for helium, and 1.42 to 2.21% for carbon dioxide. Thus, we are able to set the threshold values for He and CO_2 at 5.28–5.34 ppm and 2.49–4.23%, respectively which enabled us to recognize anomalous values for each profile.

Figure 2 shows the He and CO_2 results for each of the 18 profiles. Some anomalously high concentrations, up to 5.6 ppm and 12% for He and CO_2, respectively, can be found at specific positions along each of 18 profiles. We observe that both high He and CO_2 concentrations occurred at the same site of most profiles. Assuming that those anomalous high concentration gases mainly come from deep-crustal sources through the faults/fractures zone, they can be explained well by the advection model via CO_2 serving as the carrier gas to bring the trace gas, helium, to the surface. Therefore, it can be inferred that those sites may be the surface trace of faults/fractures zone in this area.

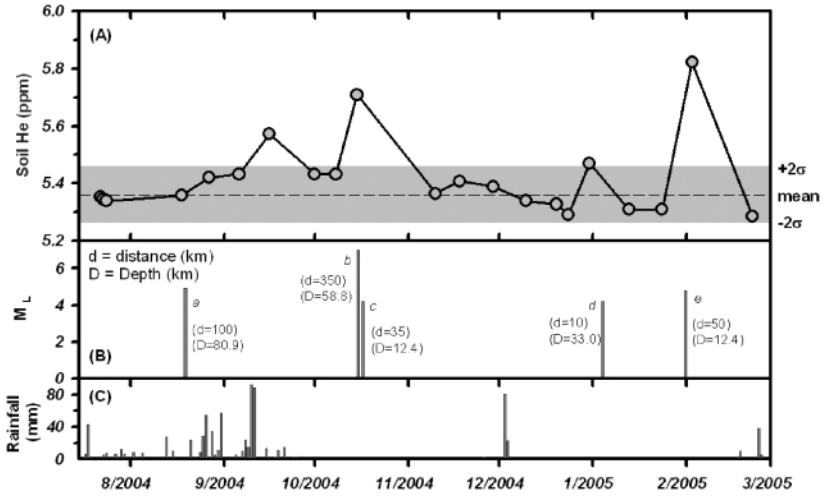

Fig. 4. Variations of average helium concentrations of point 5 and 6 along the profile I (Figs. 1B and 3) during the time period 22nd July 2004 to 3rd February, 2005. Dash line and shadowed area indicate the mean and threshold (mean ±2σ) of the helium concentration of the profile. It is interesting to note that the helium concentration in soil gas seems not affected by the rainfall, nevertheless, it is closely related to the earthquake (see discuss in the text).

It is interesting to note that, however, some of the high concentration sample sites do not simultaneously exhibit both high He and CO_2 concentration. It suggests that there are, in addition to the deep-crustal source component, multiple sources for those high concentration gases. Gas sources of the studied samples will be further discussed in later section.

Temporal variations of soil gases

In order to examine the temporal variations of soil gases, profile I was chosen for continuous sampling during the period from 22nd July, 2004 to 10th November, 2004 (Fig. 3). In Fig. 3, sampling was done for three consecutive days, i.e., 22–24 July, 2004, as marked by day-1, -2, and -3. In this three-day period, no significant variations of the helium and carbon dioxide concentrations were observed. More importantly, the anomalous high concentrations always occurred at the same sites of the profile. This indicates that the soil gas compositions do not show significant variations within short period, i.e., a few days, although CO_2 concentrations were found to be higher than earlier data from the same profile I shown in Fig. 2B. Data for day-4 to day-7 (Fig. 3) were obtained in subsequent months (August to October, 2004). Compared with day-1 to day-3, no major changes were observed for day-4, whereas, on day-5, both helium and carbon dioxide concentrations showed an increase. Day-6 represents sampling right after an earthquake (event b in Fig. 4) occurred on the same day and is characterized by a clear increase in helium concentrations. In contrast, carbon dioxide concentrations decreased. Four weeks later, i.e., on day-7, helium concentration gradually returned to the original values but carbon dioxide concentration did not increase to the original values. Comparison of the above seven profiles thus suggests that an earthquake and/or local stress may change the degassing-system and, the concentrations of soil gases would vary at different time at the same position.

In order to evaluate the variation of helium concentration as a result of tectonic activities, the mean value of points 5 and 6 along profile-I, shown in Fig. 3, has been calculated for the period from 22nd July, 2004 to 1st March, 2005 (Fig. 4). From the time series variation shown in Fig. 4, the meteorological factor, i.e., rainfall, is not the major factor to affect the variations of soil helium gas. However, the helium anomalies seem to be related to the earthquake events. An earthquake (event a in Fig. 4) on 19th August, 2004 did not cause conspicuous variation of helium concentration, perhaps due to the fact that the epicenter of the earthquake was located too far away from the study area (*ca*. 100 km) and/or that the hypocenter of the earthquake was too deep (*ca*. 81 km). Helium concentrations showed high values on 16th September, 2004 but there was no earthquake. This could be related to other crustal activity in study area. Higher values of helium concentration were recorded a few hours after the magnitude 7.0 earthquake (event b in Fig. 4) of 15th October, 2004, however, one day before the local earthquake (event c in Fig. 4) of 16th October, 2004. Because no data could be obtained for next three weeks, the duration of this anomalous trend can not be established. A precursory increase in the helium concentration of helium in the subsurface soil prior to earthquake (event d in Fig. 4) on 4th January, 2005 has been recorded on 31st

December, 2004. Highest value of helium concentration was recorded after an earthquake (event e in Fig. 4) on 31 January, 2005. These results suggest that earthquakes may affect the degassing-system of soil gases during similar meteorological condition. And hence, the site may be sensitive to the local crustal stress and thus suitable for continuous monitoring.

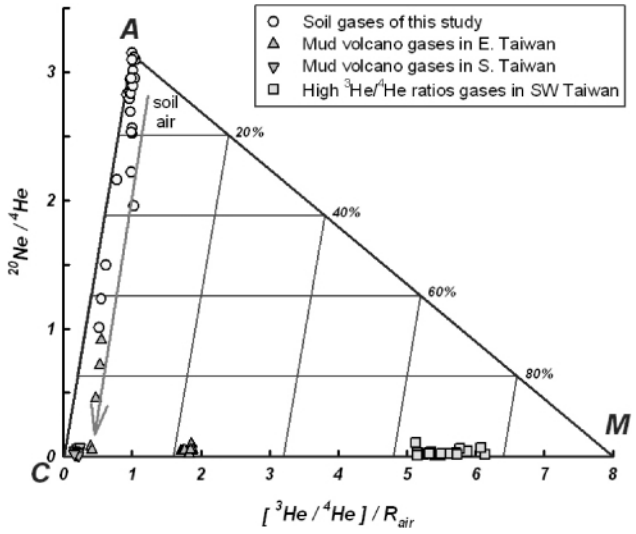

Fig. 5. Three-component plot of helium isotopes of representative soil gas samples around the Chaochou Fault. Gas samples from mud volcanoes in southern Taiwan are shown for comparison (data source from Yang et al., 2003a, b). A: air; C: crust; M: mantle component.

Sources of the soil gases

Terrestrial materials exhibit a wide of helium isotopic ratios from 0.01 to 40 times of the $^3He/^4He$ ratio of the air (*Ra*). Hence, the helium isotopic ratio is widely used as a useful tool to trace the relevant samples source domain (e.g., Ozima and Podosek, 2002; Porcelli *et al*., 2002). The helium isotopic ratios measured in this study range from 7.17×10^{-7} to 1.46×10^{-6} (i.e., 0.52 to 1.05 *R*/*Ra*) (Table 1), which illustrates that most samples contain an atmospheric air component without signature of mantle component (Fig. 5). Unlike the compositions of mud volcano gases from Southwest and East Taiwan, which exhibit distinct mantle and crustal signatures (Yang *et al*., 2003a, 2003b, 2004), most analyzed soil samples in this study are dominant with air composition as shown in the diagram of on the three-component plot (Fig. 5). Furthermore, some samples appear to contain a significant crustal component which might migrate toward the surface through the fault/fracture zones from their deep crustal source. Carbon isotopic data for carbon dioxide in the soil samples range from –11.8 to –23.4‰ PDB (Table 1), which may be interpreted as the result of mixing between organic sediments (*ca*. –30‰) and limestone (0‰) components, since the mantle component has been ruled out based on helium isotopic data.

Trace gases like radon, helium etc., besides moving by diffusion, usually can migrate toward the surface from deep sources together with other gases, e.g., CO_2 and CH_4, which are called carrier gases (Etiope and Martinelli, 2002; Yang *et al*., 2003b). As shown in Fig. 6, in addition to the air component "A", which is the dominant source for soil gas, two other end components can be identified. One is the deep source component "B", in which helium

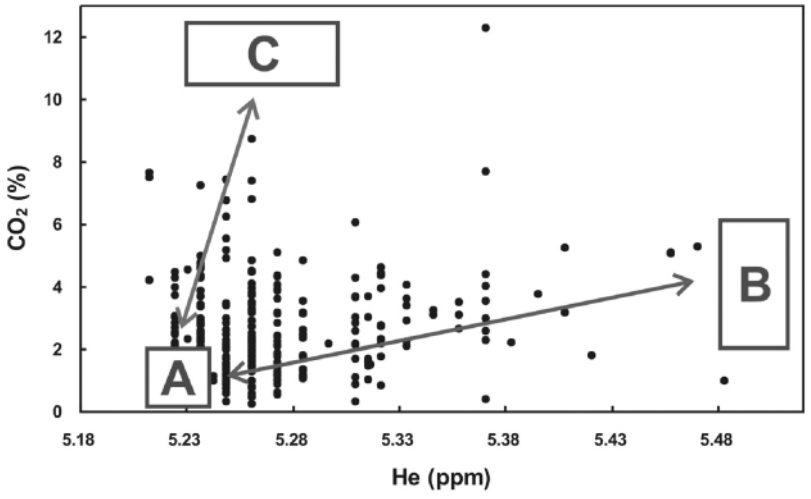

Fig. 6. Variation diagram of He versus CO_2 compositions of soil gas. At least three end members can be identified: (A) air component with low He and CO_2; (B) deep source component with high both He and CO_2; (C) shallow source component with high CO_2 but low He concentrations.

Table 1. Compositions[a] of representative gases from soil gas samples in Pingtung area, Taiwan

Sample No.	Ar + O_2 (%)	N_2 (%)	CO_2 (%)	$^4He/^{20}Ne$	$^3He/^4He$ ($\times10^{-6}$)	$[Ra \pm 1\sigma]^b$	$[^4He]$ (ppm)	$\delta^{13}C$ (‰)
P1	17.84	80.44	1.72	0.340	1.532	0.97 ± 0.01	5.36	–20.64
P2	10.36	84.77	4.88	—	—	—	5.46	–16.07
P3	18.19	81.40	0.42	—	—	—	5.32	–17.81
P4	12.60	83.56	3.84	—	—	—	5.40	–15.85
P5	16.61	81.37	2.02	0.318	1.391	1.00 ± 0.02	5.26	–19.17
P6	8.42	83.65	7.93	0.332	1.405	1.01 ± 0.02	5.41	–15.39
P7	16.17	80.37	3.47	0.323	1.458	1.05 ± 0.08	5.33	–19.80
P8	19.38	80.63	0.00	0.390	1.395	1.00 ± 0.02	5.35	–18.56
P9	19.15	79.51	1.34	0.372	1.351	0.97 ± 0.01	5.30	–11.77
P10	13.39	82.15	4.46	0.354	1.299	0.93 ± 0.01	5.35	–22.62
P11	11.86	82.18	5.96	0.358	1.336	0.96 ± 0.01	5.33	–20.75
P12	14.40	82.79	2.81	0.352	1.338	0.96 ± 0.01	5.35	–20.96
P13	14.27	81.93	3.80	0.339	1.440	1.04 ± 0.03	5.33	–19.93
P14	15.37	80.19	4.44	0.321	1.427	1.03 ± 0.01	5.25	–17.08
P15	7.95	84.41	7.64	0.451	1.377	0.99 ± 0.02	5.32	–20.01
P16	15.52	82.41	2.07	0.353	1.355	0.98 ± 0.01	5.40	–17.67
P17	14.28	81.60	4.12	0.397	1.396	1.00 ± 0.02	5.37	–15.83
P18	17.39	80.83	1.79	0.346	1.405	1.01 ± 0.02	5.33	–16.19
P19	22.35	75.48	2.17	0.395	1.372	0.99 ± 0.02	5.30	—
P20	19.31	77.58	3.10	0.339	1.379	0.99 ± 0.01	5.35	—
P21	5.79	85.45	8.76	0.323	1.384	1.00 ± 0.01	5.27	
P22	17.32	75.88	6.80	0.511	1.416	1.02 ± 0.01	5.25	—
P23	17.69	79.26	3.05	0.463	1.086	0.78 ± 0.00	5.43	–20.18
P24	12.20	80.12	7.68	0.813	0.765	0.55 ± 0.00	5.35	—
P25	7.51	80.18	12.31	0.670	0.860	0.62 ± 0.00	5.31	–23.40
P26	20.33	76.82	2.86	0.995	0.717	0.52 ± 0.00	5.27	—

[a]Major compositions were carried out using a portable micro gas chromatography with a TCD detector and helium as carrier gas; typical analytical error is less than 5%. Helium concentrations were analyzed with a helium leak detector mass spectrometer, with air as a routine standard; the typical errors are about 0.3%. Helium and carbon isotopic ratios were analyzed with mass spectrometer as described in the text.
[b]Ra is the $^3He/^4He$ ratio of air (1.39×10^{-6}).

is carried by carbon dioxide so that helium concentrations rise as carbon dioxide concentrations increase. The other one is the shallow source component "C", in which helium concentrations do not show distinct variation as carbon dioxide concentrations increase. This is evidence that soil carbon dioxide in the region originates from both shallow and deep components.

Spatial variations of soil gases and recognition of trace of fault/fracture

Many faults have been recognized in the region, including the CC Fault, and the Pingdingshan (PDS) and CY Fault as shown in Fig. 1C, and also the proposed WL Fault which is located at southwest of the CC Fault and not shown in the Fig. 1. However, the distribution, extension and characteristics of those faults are not clear at present because only very few surface traces of those faults can be precisely examined. Nevertheless, all available evidence, including geomorphological, geological, and geophysical data, support that the major structures in the region are mainly distributed in the N-S direction (Fig. 1C). Therefore, the soil gas data can help to recognize the actual location of faults and fractures in this area. Based on the distribution of anomalous high helium and carbon dioxide values (Fig. 2), the distribution of faults and fractures distribution in the studied area can be drawn (Fig. 7).

Comparing the structural lines based on helium data with those based on carbon dioxide data (Fig. 7), it is seen that both show similar/identical distribution and a N-S trend. It suggests that both helium and carbon dioxide are useful index gases for the location of faults, even though in details, a few lines are not completely consistent in some locations. Anomalous carbon dioxide data may originate not only from deep sources but also from shallow sources as discussed previously. Hence, soil helium anomalies are considered as the major index in this study.

Four major fault zones can be recognized from both helium (Fig. 7A) and carbon dioxide (Fig. 7B) results. Compared with topographic data (Shih *et al.*, 1984), lineations of soil gas anomalies "b" and "f", "d" and "h", "c" and "g" shown in Fig. 7 may correspond to the CC Fault, PDS Fault and CY Fault, respectively (as shown in

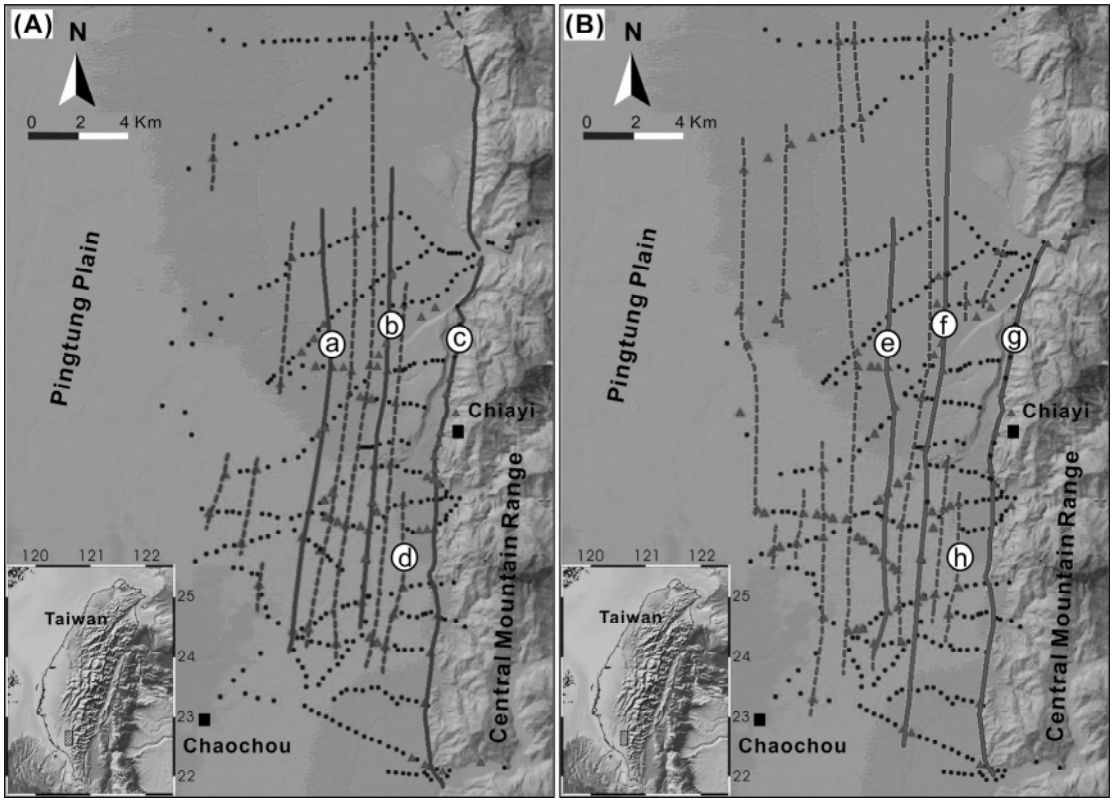

Fig. 7. Distribution of fault and fracture patterns recognized in studied area by (A) helium data; (B) carbon dioxide data. Line a and e: the Wanlong Fault; line b and f: the Chaochou Fault; line c and g: the Chiayi Fault; line d and h: the Pingdingshan Fault (see discussion in the text).

Fig. 1C); and those of "a" and "e" would be the WL Fault. In addition, some unknown structural lines may be distributed in this area. The Central Geological Survey proposed that the CC Fault is located on an obvious topographical characteristic boundary between the Pingtung Plain and the Central Mountain Ranges (location C as indicated with an arrow in Fig. 1D) (Lin *et al*., 2000). However, Chang (1986) considered that the CC Fault site should be located westward because the surface was covered with stepped terraces (location A as indicated with an arrow in Fig. 1D). Gas compositions show anomalous values at the boundary of topography but not highest helium and carbon dioxide concentrations. This zone of anomalous values (line c and g in Fig. 7) may imply the presence of a fault (the CY Fault in Fig.1C), which resulted from the back thrust of CC Fault toward surface.

Soil gas compositions are closely related to porosity and composition of soil. Assuming that no significant differences in the chemical composition of the underneath bed rock at both sides of the fault/fracture exist; anomalous gas concentrations for sandy soils (Fig. 8A) will be higher than muddy soils (Fig. 8B) due to differences of porosity and permeability between sandy and muddy soils. Whereas, gravel soils with greater porosity could show very small anomaly, even where faults/fractures do exist underneath, due to air contamination and dilution by atmospheric air (Fig. 8C). Analytic results from the profiles in Fig. 2 show that the distribution of anomalous soil gas compositions may not only result from a main fault and/or fracture as shown in Figs. 8A, 8B and 8C. Distribution of anomalous soil gas compositions illustrated the presence of several faults/fractures (Figs. 8D, 8E and 8F) in the study area.

Combining the above-mentioned data with other geological information, we can derive a simple model which illustrates the tectonic features of the study area (Fig. 9). From the proposed model it has been found that there is a main deep rupture of the CC Fault, when extended toward a shallow position, forked into three faults, i.e., the WL Fault, the CC Fault and the CY Fault, respectively (line a, b and c in Fig. 7A; and line A, B, C in Fig. 9). In addition to the three major faults, many fracture zones could also exist. Further geological and geophysical investigations, including studies of trenches and by drilling, would be necessary to verify the subsurface structures in the area.

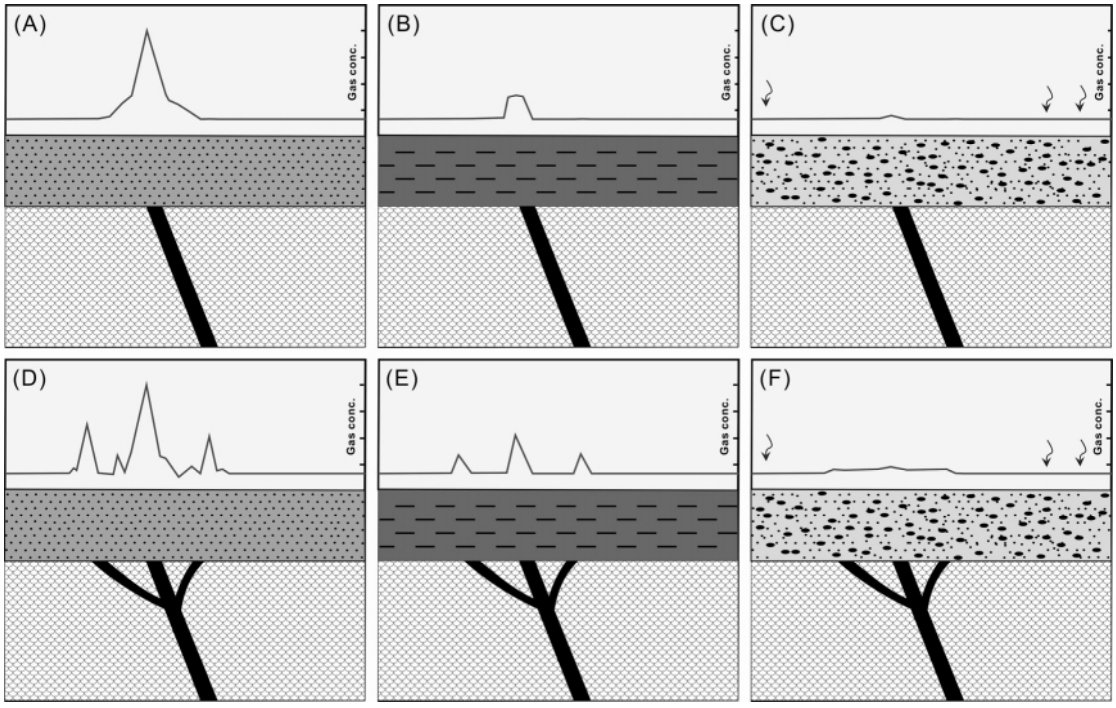

Fig. 8. Sketch of anomalous distribution of soil gases for different types of soils overlain on single and many fault zones. (A) and (D) show that sandy soils with higher porosity, usually show much clearer anomalies. In contrast, (B) and (E) show smaller anomaly for muddy soils with lower porosity. (C) and (F) indicate that very small anomaly may occur, even faults do exist underneath, for soils with gravels due to the severe air contamination and dilution.

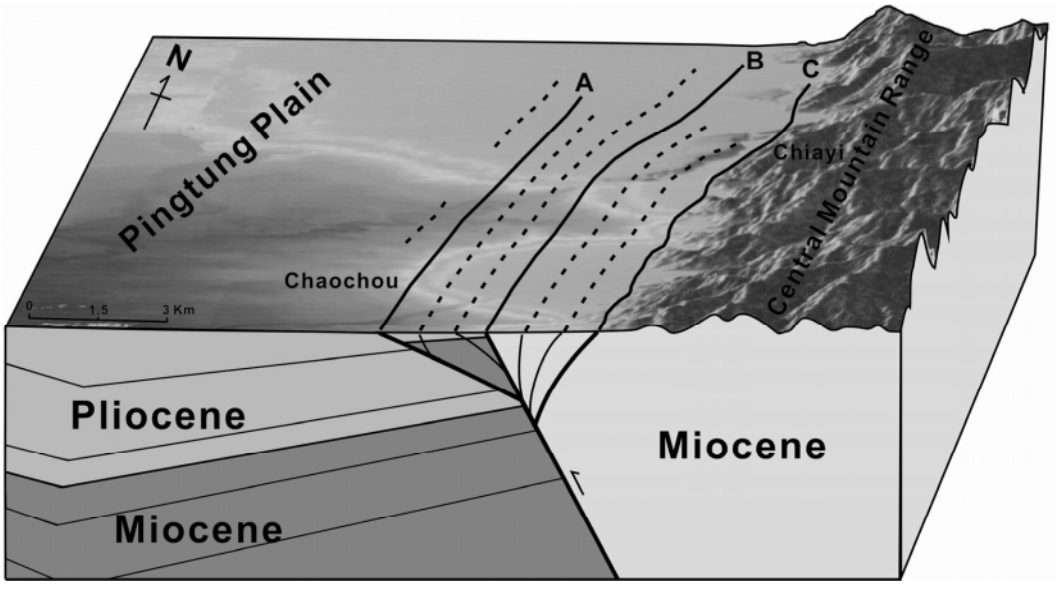

Fig. 9. Sketch 3-D tectonic model of the study area interpreting the geochemical result and including the geological, geophysical and geomorphological data in SW Taiwan. Three major faults can be recognized in the region: A: the Wanlong Fault; B: the Chaochou Fault; C: the Chiayi Fault. Some fracture zones may also exit near the surface.

CONCLUSION

The soil gas method has been applied to trace buried faults in southern Taiwan. The results show that, in the present case, helium and carbon dioxide are reliable and sensitive indicators for tracing faults than other gases. In the profiles studied, the peak concentrations recorded on the fault trace were higher than the background values. Helium and carbon dioxide soil gas anomalies were found to be linearly distributed along the N-S trends and agree well with those known from earlier studies. Hence, the soil gas method is considered to be suitable tool for the exploration of buried faults and/or fractures, at least in SW Taiwan.

Three components are required to explain the He and CO_2 concentrations and He-C isotopic ratios of soil gases. Besides the dominant atmospheric air component, a deep crustal gas component, exhibiting both high He and CO_2 concentration, is considered as good indicator of trace of deep faults/fractures in the area. The other gas component, exhibiting high CO_2 and low He concentration, may be derived from shallow depth and may not be sensitive to the deep faults/fractures.

Continuous monitoring along a selected profile indicates that an earthquake or crustal activity may affect the degassing-system during similar to meteorological conditions. Continuous monitoring, therefore, is necessary to further clarify the relationship between soil gas variations and fault activities in the area.

Acknowledgments—Thanks are due to Messrs. K. W. Wu, W. L. Hong, H. F. Lee, T. F. Lan, D. R. Hsiao, B. W. Lin and C. C. Wang at the Department of Geosciences of NTU for help with collecting and analyzing samples. Dr. Y. G. Chen kindly offered facility and help for carbon isotopes analysis. Drs. C. H. Chou and J. Du helped in the administrational arrangement to sample in NPUST campus. Drs. W. S. Chen, J. C. Hu, Y. M. Wu, Y. G. Chen, C. H. Lo of this department and C. W. Lin of Central Geological Survey gave valuable suggestions in this work. Drs. U. Knittel and L. L. Chyi gave critical comments and improved the manuscript. The National Science Council financially supported this research (TFY/92-2116-M-002-003; 93-2119-M-002-027).

REFERENCES

Al-Hilal, M. and Mouty, M. (1994) Radon monitoring for earthquake prediction on Al-Ghab of Syria. *Nuclear Geophysics* **8**, 291–299.

Baubron, J.-C., Rigo, A. and Toutain, J.-P. (2001) Soil gas profiles as a tool to characterize active tectonic areas: the Jaut Pass example (Pyrenees, France). *Earth Planet. Sci. Lett.* **196**, 69–81.

Belt, J. Q., Jr. and Rice, G. K. (2002) Application of statistical quality control measures for near-surface geochemical petroleum exploration. *Computers & Geosciences* **28**, 243–260.

Blunt, M., Fayers, F. J. and Orr, F. M. (1993) Carbon dioxide in enhanced oil recovery. *Energy Conversion and Management* **34**, 1197–1204.

Butt, C. R. M. and Gole, M. J. (1986) Groundwater helium surveys in mineral exploration in Australia. *J. Geochem. Explor.* **25**, 309–344.

Chang, H. C. (1986) Neotectonic study of the northern Chaochou fault in southern Taiwan. MS thesis, National Taiwan Univ., Taipei, 60 pp. (in Chinese).

Chen, W. S., Liu, L. H., Yan, Y. C., Yang, H. C., Lee, L. S., Yu, N. T., Chang, H. C., Shih, R. C., Chen, Y. G., Lee, Y. H., Lin, W. H., Shih, T. S. and Lu, S. T. (2003) Paleoseismologic study of the Hsincheng Fault. *Spec. Publ. Cent. Geol. Survey* **14**, 11–24 (in Chinese with English abstract).

Chen, W. S., Yang, C. C., Yang, H. C., Yu, N. T., Chen, Y. C., Wu, L. C., Lin, C. W., Chang, H. C., Shih, R. C. and Lin, W. H. (2004) Geomorphic characteristics of the Mountain-Valley in the subsidence environment of the Taipei Basin, Langyang Plain and Pingtung Plain. *Bull. Cent. Geol. Survey* **17**, 79–106 (in Chinese with English abstract).

Chiang, S. C. (1971) Seismic study of the Chaochou strucrure, Pingtung, Taiwan. *Petrol. Geol. Taiwan* **8**, 281–294.

Chyi, L. L., Chou, C. Y., Yang, T. F. and Chen, C-H. (2002) Automated radon monitoring of seismicity in a fault zone. *Geofisica Internacional* **41**(4), 507–511.

Chyi, L. L., Quick, T. J., Yang, T. F. and Chen, C-H. (2005) Soil gas radon spectra and earthquakes. *Terr. Atmos. Oceanic Sci.* **16**, 763–774.

Ciotoli, G., Etiope, G., Guerra, M. and Lombardi, S. (1999) The detection of concealed faults in the Ofanto Basin using correlation between soil-gas fracture survey. *Tectonophysics* **301**, 321–332.

Corazza, E., Magro, G., Pieri, S. and Rossi, U. (1993) Soil gas survey in the geothermal area of Bolsena Lake (Vulsini Mountains, central Italy). *Geothermics* **22**, 201–214.

Etiope, G. and Lombardi, S. (1995) Evidence for radon transport by carrier gas through faulted clays in Italy. *J. Radioanaly. Nucl. Chem.* **193**, 291–300.

Etiope, G. and Martinelli, G. (2002) Migration of carrier and trace gases in the geosphere: an overview. *Phys. Earth Planet. Inter.* **129**, 185–204.

Fytikas, M., Lombardi, S., Papachristou, M., Pavlides, S., Zouros, N. and Soulakellis, N. (1999) Investigation of the 1867 Lesbos (NE Aegean) earthquake fault pattern based on soil-gas geochemical data. *Tectonophysics* **308**, 249–261.

Gole, M. J., Butt, C. R. M. and Snelling, A. A. (1986) A groundwater helium survey of the Koongarra uranium deposits, Pine Creek Geosyncline, Northern Territory. *Uranium* **2**, 343–360.

Gregory, R. G. and Durrance, E. M. (1985) Helium, carbon dioxide and oxygen soil gases: small-scale variation over fractured ground. *J. Geochem. Explor.* **24**, 29–49.

Guerra, M. and Lombardi, S. (2000) Soil-gas method for tracing neotectonic faults in clay basins: the Pisticci field (Southern Italy). *Tectonophysics* **339**, 511–522.

Hinkle, M. E. (1978) Helium, mercury, sulphur compounds and carbon dioxide in soil gases of the Puhimau thermal area, Hawaii Volcanoes National Park, Hawaii. US Geol. Survey, Open-file Report 14, 78-246.

Hsieh, P. S. (2000) The gas sources of hot springs and mud volcanoes in Taiwan. MS thesis, Inst. Geosciences, National Taiwan Univ., 77 pp. (in Chinese with English abstract).

Hsieh, S. H. (1970) Geology and gravity anomalies of the Pingtung plain, Taiwan. *Proc. Geol. Soc. China* **13**, 76–89.

Hu, J. C., Yu, S. B., Angelier, J. and Chu, H. T. (2001) Active deformation of Taiwan from GPS measurements and numerical simulations. *J. Geophys. Res.* **106**, 2265–2280.

Huang, M. T., Pan, K. L. and Yen, T. P. (1986) Active fault study of the Taoyuan-Hsinchu area (1). National Science Council Prevention Science and Technology Report, No. 74-39.

King, C. Y. (1980) Episodic radon changes in subsurface soil gas along active faults and possible relation to earthquakes. *J. Geophys. Res.* **85**, 3065–3078.

Lee, J. C., Chen, Y. G., Sieh, K., Mueller, K., Chen, W. S., Chu, H. T., Chan, Y. C., Rubin, C. and Yeats, R. (2001) A vertical exposure of the 1999 surface rupture of the Chelungpu Fault at Wufeng, Western Taiwan: structural and paleoseismic implications for an active thrust fault. *Bull. Seism. Soc. Am.* **91**, 914–929.

Lin, C. W., Chang, W. C., Lu, S. T., Shih, T. S. and Huang, W. C. (2000) An introduction to the active faults of Taiwan. 2nd edition. *Spec. Publ. Cent. Geol. Surv*ey **13**, 1–122.

Lin, C. W., Shih, R. C., Lin, Y. H. and Chen, W. S. (2002) Structural characteristics of the Chelungpu fault zone in the Taichung area, central Taiwan. *Western Pacific Earth Sciences* **2**, 411–426.

Ozima, M. and Podosek, F. A. (2002) *Noble Gas Geochemistry*. 2nd ed., Cambridge University Press, Cambridge, 286 pp.

Porcelli, D., Ballentine, C. J. and Wieler, R. (2002) An overview of noble gas-geochemistry and cosmochemistry. *Noble Gases in Geochemistry and Cosmochemistry* (Porcelli, D. *et al*., eds.), *Reviews in Mineralogy and Geochemistry* **47**, 1–19.

Reimer, G. M. (1980) Use of soil-gas helium concentrations for earthquake prediction: limitations imposed by diurnal variations. *J. Geophys. Res.* **85**, 3107–3144.

Reimer, G. M. and Otton, J. K. (1976) Helium in soil gas and well water in the vicinity of a uranium deposit, Weld County, Colorado. US Geol. Survey, Open-file Report 76-699, 10 pp.

Roberts, A. A., Friedman, I., Donovan, T. J. and Denton, E. H. (1975) Helium survey, a possible technique for locating geothermal reservoirs. *Geophys. Res. Lett.* **2**, 209–210.

Shih, T. T., Teng, K. H., Chang, J. C., Yang, G. S. and Hsu, M. Y. (1984) Geomorphological study of active faults in western and southern Taiwan. *Research Report of Department of Geography, National Taiwan Normal Univ.* **10**, 49–94.

Shih, T. T., Teng, K. H., Chang, J. C., Shih, C. D. and Yang, G. S. (1986) Geomorphological study of active faults in Taiwan. *Research Report of Department of Geography, National Taiwan Normal Univ.* **12**, 1–44.

Sugisaki, R. (1983) Origin of hydrogen and carbon dioxide in fault gases and its relation to fault activity. *J. Geol.* **91**, 239–258.

Toutain, J.-P. and Baubron, J.-C. (1999) Gas geochemistry and seismotectonics: a review. *Tectonophysics* **304**, 1–27.

Virk, H. S. and Singh, B. (1993) Radon anomalies in soil-gas and groundwater as earthquake precursor phenomena. *Tectonophysics* **227**, 215–224.

Walia, V., Su, T. C., Fu, C. C. and Yang, T. F. (2005a) Spatial variations of radon and helium concentrations in soil gas across Shan-Chaio fault, Northern Taiwan. *Radiat. Meas.* **40**, 513–516.

Walia, V., Virk, H. S., Yang, T. F., Mahajen, S., Walia, M. and Bajwa, B. S. (2005b) Earthquake prediction studies using radon as a precursor in N-W Himalayas, India: a case study. *Terr. Atmos. Oceanic Sci.* **16**, 775–804.

Wang, S. (1976) ERTS-1 satellite imagery and its application in regional geologic study of southwestern Taiwan. *Petrol. Geol. Taiwan* **13**, 37–57.

Weng, P. S. (1988) Using variation of radioactive radon concentration in soil for research on the Chinshan fault. National Science Council Prevention Science and Technology Report, No. 77-14 (in Chinese).

Yang, T. F., Chen, C-H., Tien, R. L., Song, S. R. and Liu, T. K. (2003a) Remnant magmatic activity in the Coastal Rang of East Taiwan after arc-continent collision: fission-track date and $^{3}He/^{4}He$ ratio evidence. *Radiat. Meas.* **36**, 343–349.

Yang, T. F., Chou, C. Y., Chen, C-H., Chyi, L. L. and Jiang J. H. (2003b) Exhalation of radon and its carrier gases in SW Taiwan. *Radiat. Meas.* **36**, 425–429.

Yang, T. F., Yeh, G. H., Fu, C. C., Wang, C. C., Lan, T. F., Lee, H. F., Chen, C-H., Walia, V. and Sung, Q. C. (2004) Composition and exhalation flux of gases from mud volcanoes in Taiwan. *Environ. Geol.* **46**, 1003–1011.

Yang, T. F., Lan, T. F., Lee, H. F., Fu, C. C., Chuang, P. C., Chen, C-H., Chen, C. T. A. and Lee, C. S. (2005a) Gas compositions and helium isotopic ratios of fluid samples around Kueishantao, NE offshore Taiwan and its tectonic implications. *Geochem. J.* **39**, this issue, 469–480.

Yang, T. F., Walia, V., Chyi, L. L., Fu, C. C., Wang, C. C., Chen, C-H., Liu, T. K., Song, S. R., Lee, C. Y. and Lee, M. (2005b) Variations of soil radon and thoron concentrations in a fault zone and prospective earthquakes in SW Taiwan. *Radiat. Meas.* **40**, 496–502.

Yu, S. B., Yeh, Y. T. and Tsai, Y. B. (1983) Microearthquake activity in southwestern Taiwan. *Bull. Inst. Earth Sci. Academica Sinica* **3**, 71–85.